24. Hesselbo, S. P. *et al.* Massive dissociation of gas hydrate during a Jurassic oceanic anoxic event. *Nature* **406,** 392–395 (2000).
25. Kvenvolden, K. A. in *Gas Hydrates: Relevance to World Margin Stability and Climate Change* (eds Henriet, J. P. & Mienert, J.) 9–30 (Spec. Publ. 137, Geological Society of London, 1998).
26. Hoffman, P. F., Halverson, G. P. & Grotzinger, J. P. Are Proterozoic cap carbonates and isotopic excursions a record of gas hydrate destabilization following Earth's coldest intervals? Comment. *Geology* **30,** 286–287 (2002).

Supplementary Information accompanies the paper on **www.nature.com/nature**.

Acknowledgements We thank S. H. Zhang, H. C. Wu, G. B. Li and D. M. Liu for field assistance, and D. Mrofka and C. Valkenburg for laboratory assistance in stable isotopic analysis. We also thank M. A. Arthur and J. P. Grotzinger for comments and suggestions. This work was supported by the NSF.

Competing interests statement The authors declare that they have no competing financial interests.

Correspondence and requests for materials should be addressed to G.J. (ganqing@mail.ucr.edu).

A change in the freshwater balance of the Atlantic Ocean over the past four decades

Ruth Curry[1], Bob Dickson[2] & Igor Yashayaev[3]

[1]*Woods Hole Oceanographic Institution, Woods Hole, Massachusetts 02543, USA*
[2]*Centre for Environment, Fisheries, and Aquaculture Science, Lowestoft, NR33 OHT, UK*
[3]*Bedford Institute of Oceanography, Dartmouth, Nova Scotia, B2Y 4A2, Canada*

The oceans are a global reservoir and redistribution agent for several important constituents of the Earth's climate system, among them heat, fresh water and carbon dioxide. Whereas these constituents are actively exchanged with the atmosphere, salt is a component that is approximately conserved in the ocean. The distribution of salinity in the ocean is widely measured, and can therefore be used to diagnose rates of surface freshwater fluxes[1], freshwater transport[2] and local ocean mixing[3]—important components of climate dynamics. Here we present a comparison of salinities on a long transect (50° S to 60° N) through the western basins of the Atlantic Ocean between the 1950s and the 1990s. We find systematic freshening at both poleward ends contrasted with large increases of salinity pervading the upper water column at low latitudes. Our results extend a growing body of evidence indicating that shifts in the oceanic distribution of fresh and saline waters are occurring worldwide in ways that suggest links to global warming and possible changes in the hydrologic cycle of the Earth.

The properties of Atlantic water masses have been changing—in some cases very much—over the five decades for which reliable and systematic records of ocean measurements are available. Careful analyses of observations have together revealed much about the magnitude, timing, and spatial scales of variability, and established a framework for interpreting the dynamics and kinematics underlying those changes[4–10]. Building upon these studies and the lengthening timeline of observations, we have evaluated the time evolution of Atlantic salinities and find evidence for long-term and large-scale changes that appear to be organized, at least in part, around the structure of the hydrologic forcing as reflected in the evaporation minus precipitation (*E–P*) distribution.

We first present the large-scale differences in salinity that arose between the late 1950s and the 1990s along a particular transect through the deep basins of the western Atlantic from 50° S to 60° N (black line in Fig. 1c). This line was chosen with some care. It spans the maxima and minima of *E–P* in both hemispheres[11,12] (Fig. 1d). As shown, the *E–P* maxima underlying the trade-wind belts north and south of the Equator are separated by a belt of net precipitation associated with the intertropical convergence zone; a third *E–P* maximum follows the axis of the Gulf Stream. The main features of the surface salinity distribution result in large part from that *E–P* distribution, so our transect crosses the regions of maximum salinity in the subtropics of both hemispheres as well as the surface salinity minima along the Equator and at both poleward ends of the line (Fig. 1c).

Figures 1b and 2b show the differences in salinity observed along this transect for the time period 1985–99 compared to 1955–69 as functions of density and depth, respectively. The corresponding average distributions of salinity along this transect for the time period 1985–99 are also shown; all are annotated to indicate the locations of water mass types to which we shall refer. Along the section as a whole (Figs 1b and 2b), we find evidence of freshening over much of the water column at both poleward extremities of the section. In the intervening tropics and subtropics, we find that the upper ocean became more saline. These changes break down as follows.

North of 40° N the Atlantic water column became fresher by approximately −0.03 p.s.u. on average, reflecting the sustained freshening of LSW (see Fig. 1 legend for names of all water masses), but also of the products of Faroe–Shetland and Denmark Strait overflow from the Nordic seas which underlie it (that is, NEADW and DSOW)[10].

Towards the southern limit of the transect, the water masses that outcrop in the regions where precipitation dominates—nominally south of 25° S in the western South Atlantic (see Fig. 1d)—have also freshened. Over the 40-yr record, the ventilated thermocline waters, in the neutral density range $\gamma_n = 25.5–27.0\,kg\,m^{-3}$, became less saline by more than −0.2 p.s.u.. The underlying AAIW and UCDW also show evidence of freshening, but at a comparatively reduced level of about −0.02 p.s.u.. A lack of deep-ocean measurements southward of 32° S in the earlier time frame precludes assessing changes below 3,000 m there.

In the waters of the tropics and subtropics, salinity increases observed over this period are greatest in the upper 500 m. Salinities increased by +0.1 to +0.4 p.s.u. over four decades in all Atlantic waters exposed to the atmosphere in the high-evaporation regions between 25° S and 35° N, corresponding to the density range $\gamma_n = 23.0–25.0\,kg\,m^{-3}$. Immediately underlying this layer, the subsurface thermocline waters in the density range $\gamma_n = 25.5–27.0\,kg\,m^{-3}$ became similarly more saline in the Northern Hemisphere. These are the SMW, whose properties are set at the sea surface in the eastern basin between 20° N and 30° N by hot, dry easterly winds from the African continent. From this source, SMW circulate westward in accordance with ventilated thermocline theory into the Caribbean and western North Atlantic[13] where they are no longer in direct contact with the atmosphere, but are easily identified by a salinity maximum at depths of 100–300 m. In the South Atlantic, by contrast, maximum salinities are found at the sea surface on the western side of the basin (see Fig. 1c).

Although rising salinities are largely a feature of the low-latitude upper ocean, we find also some increase at depth between 25° S and 40° N. Centred on the neutral density level $\gamma_n = 27.8\,kg\,m^{-3}$, these elevated salinities correspond to the mixture of Atlantic and Mediterranean water masses that occupies depths 1,200–1,500 m, immediately overlying the UNADW. A 40-yr trend towards increased salinities has been documented in the deep waters of the Mediterranean Sea[14] and the increase observed here reflects the trans-ocean spreading of that influence to the western boundary and southwards in the mid-depth Atlantic circulation. On our transect, salinity increases near $\gamma_n = 27.8\,kg\,m^{-3}$ exceed

+0.05 p.s.u. between 30° −40° N, the heart of the MOW influence at this longitude, while a lesser increase in salinity (+0.02 to +0.04 p.s.u.) can be traced at these densities southward to about 25° S.

Averaged vertically over the total water column, the observed changes in salinity—by approximately −0.03 p.s.u. north of latitude 40° N and +0.02 p.s.u. between 40° N and 25° S—are of remarkable amplitude. Taken together with the sign and pan-ocean structure of the changes, these results indicate that fresh water has been lost from the low latitudes and added at high latitudes, at a pace exceeding the ocean circulation's ability to compensate.

Although multiple factors have been implicated in these long-term changes, the available measurement record has not been sufficient to quantify their relative contributions to the observed trends, and that partitioning remains a high priority in ongoing research. The freshening of the entire system of overflow and entrainment that ventilates the deep North Atlantic has already been shown to have taken place at a remarkable, if not quite steady, rate of −0.010 to −0.015 p.s.u. per decade over the past four decades[10]. That freshening has been attributed to some combination of enhanced wind-driven exports of ice or fresh water from the Arctic, increased net precipitation rates, and elevated volumes of continental runoff from melting ice[15–18]—some of which can be associated with recent amplification of the North Atlantic Oscillation (NAO)[19]. In the low latitude Atlantic, the factors building positive salinity anomalies must also involve some combination of dynamic and thermo-dynamic processes: altered circulation, precipitation patterns and intensified trade winds[20]—themselves associated with the NAO—but also enhanced evaporation rates due to warming of the surface ocean[21].

We next examine the time history of zonally integrated salinity anomalies at 24° N—the latitude of the salinity maximum—for four density layers whose winter outcrop regions are shown in Fig. 3a. The time series in Fig. 3b documents a long-term trend of increasing salinity that bridges the time periods for which differences were shown in Figs 1 and 2. The positive anomaly is greatest (~+0.3 p.s.u.) in the 1990s and its largest contribution derives from the density layers that are most exposed to the winter

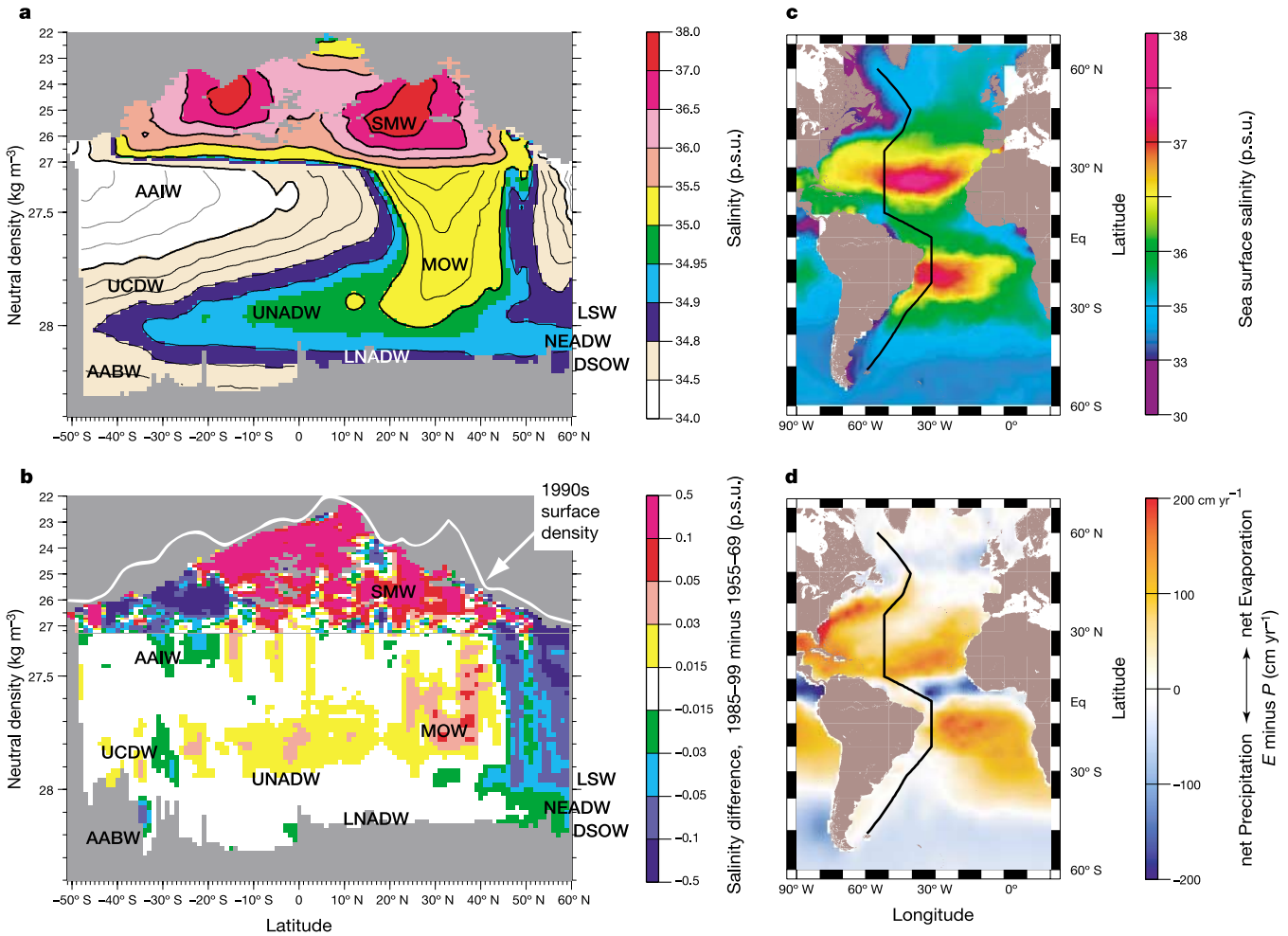

Figure 1 Western Atlantic meridional property sections and surface climatologies. **a**, Vertical section of salinity versus neutral density averaged for the years 1985–99. Grey shading means that no water at that density was measured. Annotations locate various water masses in all panels as follows. AAIW, Antarctic Intermediate Waters; UCDW, Upper Circumpolar Deep Waters; AABW, Antarctic Bottom Waters; UNADW, Upper North Atlantic Deep Waters; LNADW, Lower North Atlantic Deep Waters; MOW, Mediterranean Outflow Waters; SMW, Salinity Maximum Waters; LSW, Labrador Sea Water; NEADW, Northeast Atlantic Deep Water; DSOW, Denmark Strait Overflow Water. **b**, Salinity difference (1985–99 minus 1955–69) versus neutral density. Grey shading means that no water at that density was measured in one or both of the two time periods. No deep measurements were available south of 32° S in the earlier time frame. Sea surface densities had become considerably lighter in 1985–1999 compared to 1955–69, as depicted by the white line. No salinity difference can be computed for those surface densities, but changes at the sea surface are shown versus depth in Fig. 2. Upper-ocean density decreased in the Northern Hemisphere despite salinity increases >0.4 p.s.u., indicating that warming of the upper ocean was dominating the density changes. **c**, Climatological sea surface salinity. The black line delineates the location of the meridional section. **d**, Annual average *E*–*P* (courtesy of R. Schmitt, WHOI). p.s.u., practical salinity units.

atmosphere in the high *E–P* region along that section, that is $\gamma_n = 25.5–26.0$ and 26.0–26.5 kg m^{-3}. The deeper density layers, 26.5–27.0 and 27.0–27.5 kg m^{-3}, which outcrop northward of 30° N and 40° N respectively—away from the *E–P* maximum—show much smaller salinity changes (<+0.1 p.s.u.) over the total span of the record.

Because salt is neither gained nor lost through the atmosphere, a salinity increase in a layer implies either that additional salt (or less freshwater) was mixed in from surrounding waters, or that extra fresh water was removed. Because SMW are the most saline waters in the North Atlantic, no source for additional salt exists. Furthermore, the underlying layers exhibit no compensating freshening, so that local ocean mixing can be ruled out as the cause of the observed salinity increases. We have therefore evaluated the annual freshwater loss that could be attributed to local *E–P* changes for each of two layers, both of which are bounded above by the sea surface. The first layer considered is bounded below by the density surface $\gamma_n = 26.50$ kg m^{-3}, which includes all waters that are ventilated in the climatological *E–P* maximum south of 30° N. The second layer is bounded by a somewhat deeper surface, $\gamma_n = 27.0$ kg m^{-3}, which outcrops as far north as 40° N.

The time series of estimated *E–P* anomaly, shown in Fig. 3c, describes a basin-wide trend of enhanced freshwater loss with time in the maximum net evaporation region along 24° N. The slope of the line fitted to the time series defines the rate of estimated *E–P* change in cm yr^{-1}. Viewed as a long-term trend, the data indicate a 40-yr *E–P* increase of approximately 5 cm yr^{-1}. Alternatively, the rate of change could be characterized as an initial rise to a 20-yr plateau of ~50 cm, followed by a ~10 cm yr^{-1} increase in the 1990s. In either scenario, an additional 150–200 cm of fresh water has been

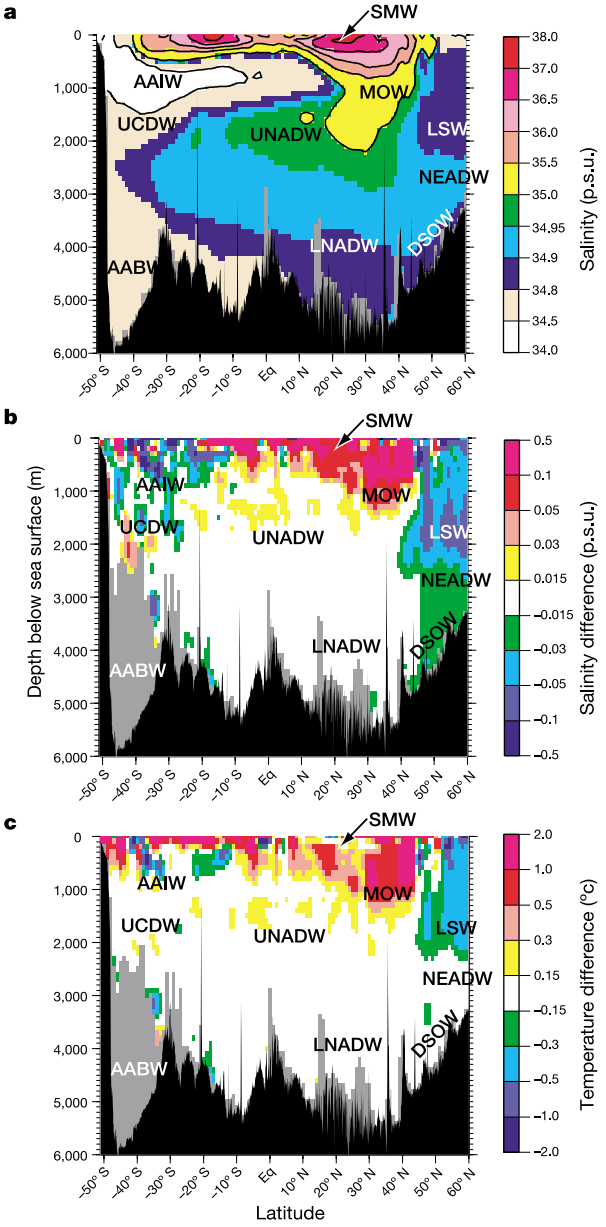

Figure 2 Western basin meridional property sections versus depth. **a**, Vertical section of salinity versus depth averaged for the years 1985–99. Water mass locations are marked as in Fig. 1. **b**, Salinity difference (1985–99 minus 1955–69) versus depth. **c**, Temperature difference versus depth for the same time periods.

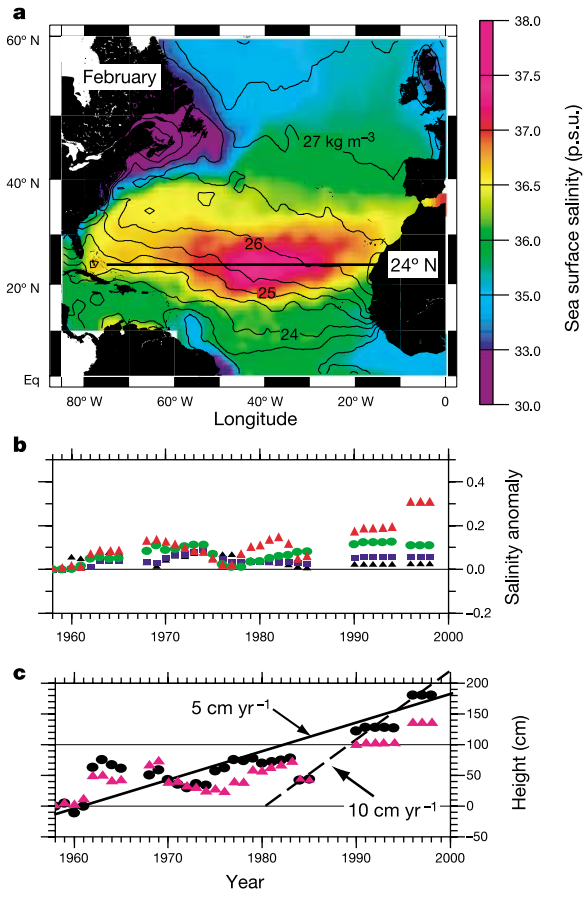

Figure 3 Time series of upper ocean salinity anomalies and estimated *E–P* anomalies. **a**, Map of February mean salinity (colour scale) and neutral density (contour interval is 0.5 kg m^{-3}) at the sea surface. The 24° N section from which time series were constructed is shown. **b**, Time series of salinity anomaly (relative to the first year in the time series) integrated across 24° N for four neutral density layers, 25.5–26.0 kg m^{-3} (red triangles), 26.0–26.5 kg m^{-3} (green circles), 26.5–27.0 kg m^{-3} (blue squares), and 27.0–27.5 kg m^{-3} (black triangles). Approximate winter outcrop regions for each layer are shown in **a**. **c**, Estimated *E–P* anomaly for two layers: sea surface to $\gamma_n = 26.5$ kg m^{-3} (magenta triangles), and sea surface to $\gamma_n = 27.0$ kg m^{-3} (black circles). Each symbol indicates the amount of extra fresh water that would have to be removed per unit area along the section to account for the observed change in salinity of that layer in each year. The slope of the line fitted to the black data points provides an estimate for the rate of change of *E–P* in cm yr^{-1}. The solid line estimates the *E–P* anomaly for the entire 42-year record span; the dashed line represents the rate of change estimated for the last 15 years. The *y* axis is the height of a column of fresh water removed by evaporation to account for the salinity change.

lost per unit area in the 1990s relative to the late 1950s. Because climatological *E–P* values are of the order of 100 cm yr^{-1} across this section, this represents a 5–10% increase in net evaporation.

The inferred 1990s rise in evaporation rate coincided with a protracted high state of the NAO. The associated increase in trade winds will have enhanced both evaporation and Ekman pumping of the SMW into the western basin's ventilated thermocline[22]. But a growing body of evidence also raises the possibility of a link to global warming and the planetary hydrologic cycle. First, tropical and subtropical upper ocean temperatures have risen in the Atlantic over the past few decades[23–25]. Temperature differences evaluated along our transect (Fig. 2c) indicate an extensive warming of the upper ocean (about 1 °C, but with the caveat that the data are not sufficient to resolve the annual heating cycle). Moreover, there is an unambiguous connection between the water masses that became more saline (Fig. 2b) and those that warmed, a feature which is confirmed by similar analyses applied to a transect through the Atlantic eastern basins. To this we add that the Clausius–Clapeyron equation[21] predicts a 5–10% increase of water vapour pressure for a temperature rise of 0.5–1.0 °C in the range 20–25 °C—similar to the order of changes in net evaporation rates we have estimated along 24° N.

In addition, parallel changes in ocean salinity and temperature distributions are occurring in other oceans. In the Mediterranean, as previously mentioned, the water masses formed by net evaporation exhibit a 40-yr trend of increasing temperature and salinity[14]. In the Pacific, a symmetric freshening of intermediate waters ventilated at high latitudes of the Northern and Southern hemispheres contrasts with zonally averaged salinity and temperature increases in the upper 200 m at several lines spanning latitudes 24° N to 32° S (ref. 26). In a subsequent analysis, the possibility that such coherent behaviour might reflect some shorter-term natural oscillation in the Pacific climate, such as the Pacific Decadal Oscillation (PDO), was discounted on the basis that recent freshening of AAIW had also been observed in the Indian Ocean where the PDO signal is slight[27,28]. An analogous argument could be extended to the hemispherically symmetric Atlantic salinity changes, to downplay the NAO as the sole dynamic at work.

Although it is a fundamental component of the planetary energy budget, the hydrologic cycle remains one of the least-understood elements of the climate system and freshwater budgets one of the largest causes for differences among climate models[29]. Given the great uncertainties in measuring evaporation and precipitation over the oceans, conclusive evidence for changes in the global water cycle will depend on present and future efforts to directly measure salinity changes and freshwater transports by ocean currents. □

Methods

Climatologies

Ocean climatologies were constructed using the HydroBase2 package[30] and its database of hydrographic profiles, which have been rigorously screened for quality. Three-dimensional fields of salinity, temperature, and neutral density at 1° grid resolution were generated for various time frames (5-, 10- and 15-yr composites) using isopycnal gridding and interpolation methods. Changes in hydrographic properties between time periods were evaluated as a function of both density and depth by subtracting identical grid points along a vertical section extracted from each climatology. Uncertainties for the data varied with time and are estimated as follows. For 1955–1969, $T = \pm 0.01$ °C and $S = \pm 0.01$ p.s.u.. For 1970–1989, $T = \pm 0.005$ °C and $S = \pm 0.005$ p.s.u.. For 1990–1999, $T = \pm 0.001$ °C and $S = \pm 0.002$ p.s.u.. Lower limits for a significant difference in salinity was set at ± 0.015 p.s.u. and for temperature at ± 0.15 °C. All of the upper-ocean signals reported here are an order of magnitude greater (0.1–0.4) than the worst-case error; and the deep-ocean anomalies exceed twice the measurement uncertainties.

Layer-averaged salinity and *E–P* anomalies

Five-year running time frames spanning the instrumental record (1955–2000) were used to estimate yearly climatologies (a 1-2-5-2-1 weighting scheme was implemented for each time frame). Time series of annual layer-averaged salinity values, S_i, for the 24° N sections were evaluated by:

$$S_i = \int\int \rho s \mathrm{d}z\mathrm{d}x \Big/ \int\int \rho \mathrm{d}z\mathrm{d}x \qquad (1)$$

where s is salinity (in p.s.u.), ρ is *in situ* density (in kg m^{-3}), dz is layer thickness (in m), and dx is the distance (in m) between successive profiles along the section. Temporal changes were defined by the difference between S_i and S_1, the first year in each time series (1958). Years for which the section contained spatial gaps exceeding 100 km after interpolation were omitted from the time series.

The freshwater loss that could be attributed to local *E–P* changes was evaluated by invoking an approximate salt conservation statement:

$$\rho_1 S_1 H = \rho_2 S_2 (H + \Delta h) \qquad (2)$$

where H is the average thickness of a layer (in cm) and Δh is the height (in cm) of fresh water removed through the air–sea boundary per unit area for each section.

Received 11 September; accepted 14 November 2003; doi:10.1038/nature02206.

1. Wüst, G. *Länderkundliche Forshung* 347–359 (Festschrift Norbert Krebs, Stuttgart, 1936).
2. Wijffels, S., Schmitt, R., Bryden, H. & Stigebrandt, A. Transport of freshwater by the oceans. *J. Phys. Oceanogr.* **22,** 155–162 (1992).
3. Lukas, R. & Lindstrom, E. The mixed layer of the Western Equatorial Pacific Ocean. *J. Geophys. Res.* **96** (suppl.), 3343–3357 (1991).
4. Levitus, S. Interpentadal variability of salinity in the upper 150m of the North Atlantic Ocean, 1970–1974 versus 1955–1959. *J. Geophys. Res.* **94,** 9679–9685 (1989).
5. Deser, C. & Blackmon, M. Surface climate variations over the North Atlantic Ocean during winter: 1900–1989. *J. Clim.* **6,** 1743–1753 (1993).
6. Bryden, H. *et al.* Decadal changes in water mass characteristics at 24°N in the subtropical North Atlantic Ocean. *J. Clim.* **9,** 3162–3186 (1996).
7. Joyce, T., Pickart, R. & Millard, R. Long-term hydrographic changes at 52 and 66°W in the North Atlantic subtropical gyre & Caribbean. *Deep Sea Res. II* **46,** 245–278 (1999).
8. Lazier, J. *et al.* in *Natural Climate Variability on Decade-to-Century Time Scales* (ed. Martinson, D. G.) 295–304 (National Academy Press, Washington DC, 1995).
9. Blindheim, J. *et al.* Upper layer cooling and freshening in the Norwegian Sea in relation to atmospheric forcing. *Deep-Sea Res. I* **47,** 655–680 (2000).
10. Dickson, R. R., Yashayaev, I., Meincke, J., Turrell, W., Dye, S. & Holfort, J. Rapid freshening of the Deep North Atlantic over the past four decades. *Nature* **416,** 832–837 (2002).
11. Schmitt, R., Bogden, P. & Dorman, C. Evaporation minus precipitation and density fluxes for the North Atlantic. *J. Phys. Oceanogr.* **10,** 1210–1221 (1989).
12. Schmitt, R. W. The ocean component of the water cycle. *Rev. Geophys.* **33,** 1395–1409 (1995).
13. Blanke, B., Arhan, M., Lazar, A. & Prevost, G. A Lagrangian numerical investigation of the origins and fates of the Salinity Maximum Water in the Atlantic. *J. Geophys. Res.* **107,** 1–15 (2003).
14. Roether, W. *et al.* Recent Changes in the Eastern Mediterranean Deep Waters. *Science* **271,** 333–335 (1996).
15. Dickson, R. R. *et al.* The Arctic Ocean response to the North Atlantic Oscillation. *J. Clim.* **13,** 2671–2696 (2000).
16. Vinje, T. Fram Strait ice fluxes and atmospheric circulation, 1950–2000. *J. Clim.* **14,** 3508–3517 (2001).
17. Peterson, B. J. *et al.* Increasing river discharge to the Arctic Ocean. *Science* **298,** 2171–2173 (2002).
18. Abdalati, W. & Steffen, K. Snowmelt on the Greenland ice sheet as derived from passive microwave satellite data. *J. Clim.* **10,** 165–175 (1997).
19. Marshall, J. *et al.* North Atlantic Climate Variability: phenomena, impacts and mechanisms. *Int. J. Clim.* **21,** 1863–1898 (2001).
20. Moulin, C., Lambert, C. E., Dulac, F. & Dayan, U. Control of atmospheric export of dust from North Africa by the North Atlantic Oscillation. *Nature* **387,** 691–694 (1997).
21. Peixoto, J. P. & Oort, A. H. *Physics of Climate* 53 (American Institute of Physics, New York, 1992).
22. Mignot, J. & Frankignoul, C. On the interannual variability of surface salinity in the Atlantic. *Clim. Dyn.* **20,** 555–565 (2003).
23. Levitus, S., Antonov, J., Boyer, T. & Stephens, C. Warming of the World Ocean. *Science* **287,** 2225–2229 (2000).
24. Joyce, T. & Robbins, P. The long-term hydrographic record at Bermuda. *J. Clim.* **9,** 3121–3131 (1996).
25. Parilla, G., Lavin, A., Bryden, H., Garcia, M. & Millard, R. Rising temperatures in the subtropical North Atlantic Ocean over the past 35 years. *Nature* **369,** 48–51 (1994).
26. Wong, A. P. S., Bindoff, N. L. & Church, J. L. Large scale freshening of intermediate waters in the Pacific and Indian Oceans. *Nature* **400,** 440–443 (1999).
27. Wong, A. P. S., Bindoff, N. L. & Church, J. C. Freshwater and heat changes in the North and South Pacific Oceans between the 1960s and 1985–94. *J. Clim.* **14,** 1613–1633 (2001).
28. Bindoff, N. L. & McDougall, T. J. Decadal changes along an Indian Ocean Section at 32S and their interpretation. *J. Phys. Oceanogr.* **30,** 1207–1222 (2000).
29. Intergovernmental Panel on Climate Change (IPCC). *Climate Change 2001: The Scientific Basis. Contribution of Working Group I to the Third Assessment Report of the IPCC* (eds Houghton, J. T. *et al.*) (Cambridge Univ. Press, Cambridge, UK, 2001).
30. Curry, R. G. *HydroBase2: A Database of Hydrographic Profiles and Tools for Climatological Analysis* ⟨http://www.whoi.edu/science/PO/hydrobase⟩ (WHOI, 2002).

Acknowledgements We are grateful to J. Toole and R. Schmitt for their encouragement and discussions. This work was supported by an NSF grant and the WHOI Ocean and Climate Change Institute. It has also formed part of the data synthesis phase of the WOCE Program, of the ASOF Project of the US NSF and the Framework V Programme of the European Community, and of the NOAA Consortium on the Ocean's Role in Climate of the Scripps Institution of Oceanography and the Lamont-Doherty Earth Observatory.

Competing interests statement The authors declare that they have no competing financial interests.

Correspondence and requests for materials should be addressed to R.C. (rcurry@whoi.edu).